

## Gold Nanobridge Stabilized by Surface Structure

Yukihito Kondo<sup>1</sup> and Kunio Takayanagi<sup>1,2</sup>

<sup>1</sup>*Takayanagi Particle Surface Project, ERATO, Japan Science and Technology Corporation, 3-1-2 Musashino, Akishima-shi, Tokyo 196, Japan*

<sup>2</sup>*Department of Material Science and Engineering, Tokyo Institute of Technology, 4259 Nagatsuta, Midori-ku, Yokohama, Kanagawa 226, Japan*

(Received 10 March 1997)

We formed gold nanowires using electron-beam irradiation in an ultrahigh vacuum electron microscope. The dimensions of these nanowires were 0.8–3 nm in thickness and 5–10 nm in length. The nanowires showed lasting stability. We propose a structure model for a nanowire with a thickness of 2 nm. The model is represented by a hexagonal prism; the surface layer of the prism has a hexagonal-close-packed (hcp) lattice, and the core of the prism has a face-centered-cubic structure. The nanowire is considered to be stabilized by the hcp lattices of the surfaces. [S0031-9007(97)04476-1]

PACS numbers: 68.35.Bs, 61.16.Bg, 61.48.+c

Recent years have brought significant advances in studies on nanoparticles and nanowires due to both theoretical and technological interests. Considerable effort has been devoted to research related to nanoparticles [1,2]. These materials are significant because their physical properties differ from bulk materials. Quantization of conductance has been attracting great interest for both theoretical and applied studies devoted to quantum devices [3]. Nanowires (i.e., atomistic contacts) prepared in a scanning tunneling microscope (STM) demonstrated the quantization of conductance even at room temperature [4–6]. However, nanowire structures have not been fully investigated because of difficulties related to their sample preparation. In previous studies, the nanowires were obtained as follows. The STM tip was driven into a sample and then pulled out. As the tip retracted, the nanocontact became a nanowire with a decrease in cross section, which broke up after milliseconds. The conductance quantization was observed from the current and voltage data obtained just before the nanowire broke up. Clearly, experimental studies require that nanowires maintain their forms stably for long periods with well-defined structure.

We successfully prepared stable gold nanowires by electron-beam irradiation on a gold thin film in an ultrahigh vacuum transmission electron microscope (UHVTEM) [7]. A question regarding how the atoms are arranged in the nanowire and on the narrow surface of the nanowire naturally arises. Such a study is a key to understanding nanostructures, where the ratio of the atoms in the surface to those in the entire structure is in the order of tens of percent. We believe that determining the structure of nanowires is fundamental in order to understand their physical properties, such as quantization of conductance. In this paper, we report the initial results of our nanowires study and describe the formation and the structure related to the surface reconstruction.

We studied gold nanowire, because the (110), (111), and (001) surfaces of gold have reconstructed structures of  $2 \times 1$ ,  $23 \times 1$ , and  $5 \times n$  ( $n = 20$  or  $28$  in previous

studies), respectively. The  $5 \times n$  structure is a hexagonal lattice registered on the square lattice of (001) layer of the bulk gold [8–12]. The  $23 \times 1$  structure is also a hexagonal lattice shrunk in the [110] direction registered on the hexagonal lattice of (111) layer [13–17].

Gold nanowires were made *in situ* at a working pressure of  $3 \times 10^{-8}$  Pa in a UHVTEM equipped with a field emission electron gun (JEOL, JEM-2000VF, 200 kV). We observed electron microscope images through a highly sensitive TV system (Gatan 622SC). The images shown in this paper were reproduced from the recorded videotape. Using electron-beam bombardment, we made nanoholes in the gold (001) film with 3 nm thickness [18–20], thereby forming a bridge such as shown in Fig. 1(a), where the beam intensity was about  $100 \text{ A/cm}^2$  and the period was around an hour. The bridge was freestanding, suspended by the Au(001) film at both ends. The bridge had the same [001] orientation as the Au(001) film, since the (200) lattice fringes of 0.204 nm had the same orientation in both the bridge and the film. When the bridge was irradiated further, the bridge became thinner. Surprisingly, every nanowire was straight and had a uniform thickness along the wire axis [see Figs. 1(b) and 2]. We obtained more than 30 nanowires, which ranged from 0.8 to 2 nm in

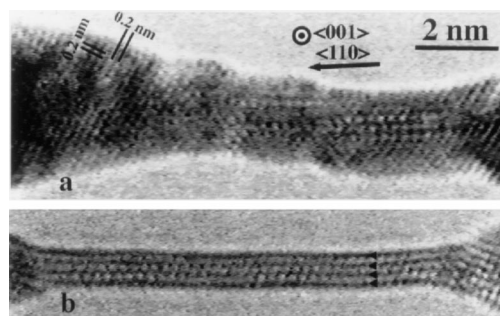


FIG. 1. Transmission electron micrographs showing the formation of a nanowire: (a) an image of Au(001) film with closely neighboring nanoholes, an initial stage of the nanowire, and (b) the thinnest nanobridge with four atomic rows.

thickness, and from 5 to 10 nm in length. The thinnest nanowire among nanowires that we observed had a width of only four atomic rows and is shown in Fig. 1(b). The thinnest nanowire remained stable under low beam intensities below  $5 \text{ A/cm}^2$ . When we applied intense irradiation (above  $100 \text{ A/cm}^2$ ) to the thinnest nanowire, it broke up after a short time (10 sec). Hereafter, we refer to the stable and straight nanowire as nanobridge (NB).

We investigated the structure of the NB using high resolution electron microscopy and electron diffraction. The electron microscope image of a NB changed as focus changed. An example of this is shown in Figs. 2(a) and 2(b), which were obtained at the focuses of +65 and +55 nm, respectively. We see a square lattice in Figs. 2(a), and a hexagonal lattice in Fig. 2(b). The hexagonal lattice appeared only around the central axis of the wire, while the square lattice appeared at both side edges of the wire. The lattice spacing of the hexagonal lattice in the  $[10]$ ,  $[01]$ , and  $[11]$  directions was directly measured at approximately 0.28 nm on the images using (200) lattice fringes of the gold film as a reference, while that of the square lattice was at about 0.2 nm. As will be shown later, we observed diffraction spots which are responsible for the square and the hexagonal lattices. We also observed Au(001) film with  $5 \times 1$  surface reconstruction, and found that hexagonal and square lattices are imaged at the focuses of 55 and 65 nm, respectively. In high resolution electron microscopy, a phase difference between diffracted and direct beams is modified depending on a focus. Contrast of the lattice image becomes weak for a phase difference of  $\pi$ . The phase differences between the corresponding diffracted waves of the hexagonal and square lattices and direct wave become  $\pi$  at the focuses of 65 and 55 nm, respectively (we used 0.7 nm for the spherical aberration

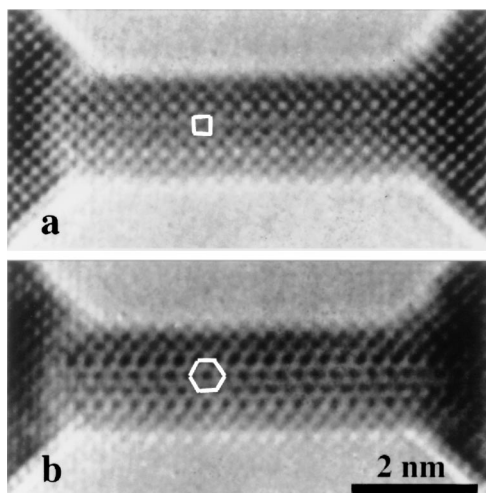


FIG. 2. Transmission electron micrographs of an NB 2 nm thick; obtained at the focuses of (a) 65 nm and (b) 55 nm. Note the square lattice in (a) and hexagonal one in (b).

of our microscope). The above explanation of the images is similar to the surface imaging technique [21,22]. Thus, the result of Figs. 2(a) and 2(b) suggests that the NB has the hexagonal lattice superimposed on the square lattice.

Diffraction patterns were obtained with probes of different sizes. An electron diffraction pattern only from an area of the NB with a 2 nm thickness is shown in Fig. 3(a). The diffraction spots are not sharp, but disk shaped, because the incident angle of the electron beam enlarges for a small probe size [23]. We also observed diffraction patterns with sharp spots from large areas of Au(001) film which suspended the NB. They showed the patterns of  $5 \times n$  structure of the reconstructed Au(001) surface. Then, we found that the disk pattern of the NB was similar to that of the reconstructed Au(001) film. One noticeable difference between the square lattice in the NB and the one in the bulk Au(001) is that the unit cell of the square lattice is not equilateral, but expanded by about 4% in the vertical direction to the wire axis. In addition, the expansion was detected in high resolution images such as Figs. 2(a) and 2(b), while the equilateral lattice images at the Au(001) film suspending the wire was observed. The reason for this expansion will be discussed later. The  $d$  values of hexagonal and square reflections in Fig. 3 are in accord with the spacings of the corresponding lattices of the electron microscope images such as in Figs. 2(a) and 2(b). The diffraction disks in Fig. 3(a) are thus interpreted to be the reflections from the hexagonal lattice and from the square lattice of the NB. As illustrated in Fig. 3(b), the  $[10]$  axis of the hexagonal lattice in real space is parallel to the wire axis, and also to the  $[10]$  axis of the square lattice.

We can observe the lattice mismatch between the hexagonal and square lattices from the diffraction

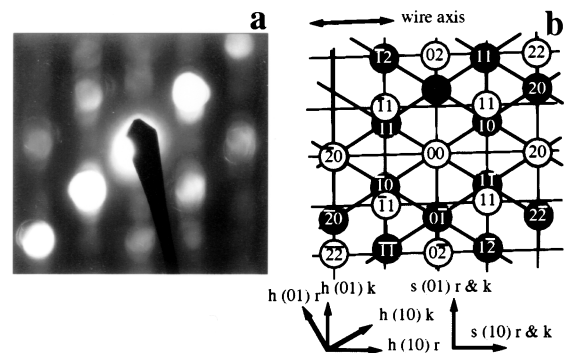


FIG. 3. (a) Electron diffraction pattern of an NB from a circular area of 2 nm, and (b) its schematic illustration. The gray circles and the open circles in (b) represent diffraction disks for a hexagonal net pattern and those for square net pattern in (a), respectively. The reflection indices  $(h, k)$  are given in the circles. The  $[10]$  axis of the hexagonal and square lattices are parallel to the wire axis indicated by an arrow. The elementary vectors of the unit cells in real and reciprocal spaces are shown below the illustration, where the  $h$  and the  $s$  indicate hexagonal and square, and the  $r$  and the  $k$  indicate real and reciprocal spaces, respectively.

patterns. The hexagonal lattice is almost coherent with the square lattice along the axis of the wire. In a vertical direction, the hexagonal lattice has a misfit with the square lattice by (20–25)%. Considering that the Au(001) surface has  $5 \times n$  structure, we may conclude that the hexagonal and square lattice correspond to the surface layer and the core of the NB, respectively.

A model of the 2 nm thick NB structure, derived from our experimental evidences and also physical considerations, is schematically shown in Figs. 4(a) and 4(b). First, we consider the wire of a face-centered-cubic (fcc) structure, which elongates along the  $[110]$  axis. The wires are bounded by  $\{001\}$  and  $\{111\}$  surfaces. Then, we reconstruct the outermost  $\{001\}$  planes to have a hexagonal-close-packed (hcp) lattice, maintaining coherency with the neighboring  $\{111\}$  surfaces in the direction of the wire axis. As a result, the wire has a hexagonal prism shape; the surface layer of the prism has a hexagonal-close-packed (hcp) lattice and the core of the prism has a face-centered-cubic structure.

Based on the model structure observations, we can explain why the electron microscope image in Fig. 2(b), shows a hexagonal lattice image around the central axis and the square lattice image on both side edges of the wire. The lattice image of the NB in Figs. 2(a) and

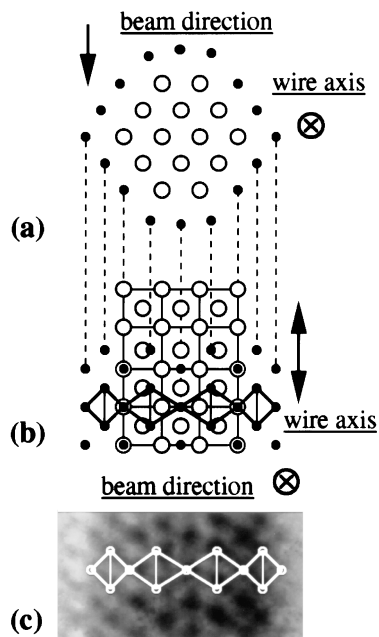


FIG. 4. Structure models of an NB 2 nm thick. (a) Sectional view of the NB. The solid circles and the open circles represent atoms in the surface layer with a hexagonal lattice and in the core of NB with an fcc structure, respectively. (b) Top view. The solid circles represent atoms in the surface layer with a hexagonal lattice. The solid circles on the (001) square lattice which is represented by the open circles were reconstructed with a two-bridge registry. The square lattice expanded in the  $[01]$  direction relative to the  $[10]$  direction. (c) The hexagonal lattice superimposed on the enlarged image of Fig. 2(b).

2(b) is periodic along the wire axis. This supports our postulation that the hexagonal lattice in the  $[10]$  direction is coherent with the square lattice in the  $[10]$  direction, which is the direction of the wire axis. The hexagonal lattice can have one of the two registries of those in  $5 \times n$  structure of the Au(001) surface: two-bridge and top/center registries (see Fig. 9 in Ref. [8]). The two-bridge registry seems to accord well with the structure of the present NB [in Figs. 2(b) and 4]. The top/center registry, on the other hand, was reported for the (001) facet plane of the multiple twinned particle [24]. The two registries depend on the number of the  $[10]$  atom rows of the hexagonal lattice on the surface and that of the square lattice in the second layer. Odd-even registry (3-2 for the model structure in Fig. 4, where the 3 is the number of atom rows in the surface and the 2 is that in the subsurface layers excluding edge atom rows) results in the two-bridge registry, and odd-odd registry (7-5 for the  $5 \times 1$  structure in Fig. 4 of Ref. [24]) results in the top/center. This is because the  $[10]$  atom rows at the edge have to maintain coherence with the neighboring  $\{111\}$  surfaces in the direction of the wire axis. The 4% expansion of the square lattice in the vertical direction to the wire axis is considered to accommodate the lattice misfit between the hexagonal and the square lattices of the two-bridge registry. It is noteworthy that the width of six hcp lattices corresponds with that of five expanded square lattices. We believe that the hexagonal lattice is relaxed so as to equilibrate the surface tensions in the section and the axial direction of a NB.

A question arises concerning the reason for the uniform thickness of the NBs. We assume that their uniformity may be related to the crystallographic orientation of the NBs. To identify the correlation between the uniformity and crystallographic orientation, we examined an NB formation from a bridge having a  $[100]$  axis. However, only a neck-shaped bridge was formed, as shown in Fig. 5. The neck-shaped bridge appeared to have the  $\{111\}$  surfaces, which were oblique with respect to the bridge axis. Thus, the generation of the  $\{111\}$  planes prevents the formation of NBs. In contrast, if the  $\{111\}$  planes extend parallel to the  $[110]$  axis to form a hexagonal prism, a straight and uniform NB is stabilized.

Finally, we briefly touch on the structure of the NB with a width of four atomic rows. The image of the NB in Fig. 1(b) shows only a hexagonal pattern. The structure of the thinnest bridge has not yet been determined.

In summary, we successfully made gold nanowires (NBs). The dimensions of the thinnest wire among NBs that we observed were only four atomic rows in width and 10 nm in length. A straight NB with a uniform thickness was formed when the wire axis was oriented along the  $[110]$  direction. The structure of NB was analyzed using high resolution electron microscopy and electron diffraction. As a result, we proposed the hexagonal prism model for a 2 nm thick NB structure,

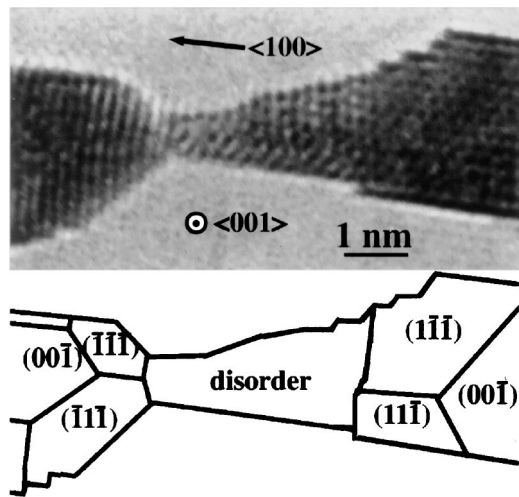


FIG. 5. A neck-shaped bridge with an axis in the  $[100]$  direction of the Au(001) films.

where the surface layers of the prism have hcp lattices and the core of the prism has expanded face-centered-cubic structure. The expansion of the fcc structure was 4% in the section direction of the NB. We also examined NB formation when the wire axis of the NB was in the  $[100]$  direction, and found that only a neck-shaped wire was formed. Finally, we concluded that a stable NB is formed, due to hcp planes which are parallel to the wire axis. A crystallographic orientation is important when constructing nanowires.

The good reproducibility and stability of the NBs is promising for experiments of the electronic transport as compare with the previously reported nanocontact. In addition, we believe that the NBs will offer opportunities for fundamental research into and potential applications

for nanostructure science. One of the authors (Y. K.) thanks Dr. Cho of their group for his kind suggestions in preparing this letter.

- 
- [1] M. Mitome, Y. Tanishiro, and K. Takayanagi, *Z. Phys. D* **12**, 45 (1989).
  - [2] S. Iijima and T. Ichihashi, *Phys. Rev. Lett.* **56**, 616 (1986).
  - [3] B. J. van Wees *et al.*, *Phys. Rev. Lett.* **60**, 848 (1988).
  - [4] N. Agrait, J. G. Rodrigo, and S. Vieira, *Phys. Rev. B* **47**, 12 345 (1993).
  - [5] J. I. Pascual *et al.*, *Phys. Rev. Lett.* **71**, 1852 (1993).
  - [6] L. Olesen *et al.*, *Phys. Rev. Lett.* **72**, 2251 (1994).
  - [7] Y. Kondo *et al.*, in *Proceedings of 13th International Congress on Electron Microscopy, Paris, 1994* (Editions de physique, Les Ulis, France, 1994), p. 269.
  - [8] M. A. Van Hove *et al.*, *Surf. Sci.* **103**, 189 (1981).
  - [9] K. Yamazaki *et al.*, *Surf. Sci.* **199**, 594 (1988).
  - [10] V. Fiorentini, M. Methfessel, and M. Schoffler, *Phys. Rev. Lett.* **71**, 1051 (1993).
  - [11] G. K. Binnig *et al.*, *Surf. Sci.* **144**, 321 (1984).
  - [12] D. Gibbs *et al.*, *Phys. Rev. B* **38**, 7303 (1988).
  - [13] J. C. Heyraud and G. J. Metios, *Surf. Sci.* **100**, 519 (1980).
  - [14] Y. Tanishiro *et al.*, *Surf. Sci.* **111**, 395 (1981).
  - [15] K. Takayanagi *et al.*, *Surf. Sci.* **205**, 637 (1988).
  - [16] V. M. Hallmark *et al.*, *Phys. Rev. Lett.* **59**, 2879 (1987).
  - [17] J. Perdureau, J. P. Biberian, and G. E. Rhead, *J. Phys. F* **4**, 798 (1974).
  - [18] D. Cherns, *Philos. Mag.* **36**, 1429 (1977).
  - [19] D. Cherns, *Surf. Sci.* **90**, 339 (1979).
  - [20] K. Niwase *et al.*, *Philos. Mag. Lett.* **74**, 167 (1996).
  - [21] W. Krakow, *Surf. Sci.* **111**, 503 (1981).
  - [22] W. Krakow, *Thin Solid Films* **93**, 235 (1982).
  - [23] J. M. Cowley, *J. Electron Microsc. Tech.* **3**, 25 (1986).
  - [24] M. Mitome and K. Takayanagi, *Phys. Rev. B* **42**, 7238 (1990).